1-1-2017

Biochemical and Biophysical Methods for Analysis of Poly(ADP-Ribose) Polymerase 1 and Its Interactions with Chromatin.

Maggie H. Chassé

Uma M. Muthurajan

Nicholas J. Clark

Michael A. Kramer
Children's Mercy Hospital

Srinivas Chakravarthy

See next page for additional authors

Recommended Citation

Chassé MH, Muthurajan UM, Clark NJ, et al. Biochemical and Biophysical Methods for Analysis of Poly(ADP-Ribose) Polymerase 1 and Its Interactions with Chromatin. Methods Mol Biol. 2017;1608:231-253. doi:10.1007/978-1-4939-6993-7_16

HHS Public Access

Author manuscript

Methods Mol Biol. Author manuscript; available in PMC 2018 January 01.

Published in final edited form as:

Methods Mol Biol. 2017 ; 1608: 231–253. doi:10.1007/978-1-4939-6993-7_16.

Biochemical and biophysical methods for analysis of Poly (ADP-Ribose) Polymerase 1 and its interactions with chromatin

Maggie H Chassé[1,*], **Uma M Muthurajan**[1], **Nicholas J Clark**[2], **Michael A Kramer**[3], **Srinivas Chakravarthy**[4], **Thomas Irving**[4], and **Karolin Luger**[1,5,6]

[1]Department of Chemistry and Biochemistry, University of Colorado at Boulder, Boulder, CO

[2]Amgen Inc., Thousand Oaks, CA

[3]Children's Mercy Hospital, Kansas City, MO

[4]BioCAT, CSRRI and Department BCS, Illinois Institute of Technology, Chicago, IL

[5]Howard Hughes Medical Institute, Chevy Chase, MD

[6]Institute for Genome Architecture and Function, Colorado State University, Fort Collins, CO

Abstract

Poly (ADP-Ribose) Polymerase I (PARP-1) is a first responder to DNA damage repair and participates in the regulation of gene expression. The interaction of PARP-1 with chromatin and DNA is complex and involves at least two different modes of interaction. In its enzymatically inactive state, PARP-1 binds native chromatin with similar affinity as it binds free DNA ends. Automodification of PARP-1 affects interaction with chromatin and DNA to different extents. Here we describe a series of biochemical and biophysical techniques to quantify and dissect the different binding modes of PARP-1 with its various substrates. The techniques listed here allow for high throughput and quantitative measurements of the interaction of different PARP constructs (inactive and automodified) with chromatin and DNA damage models.

Keywords

PARP-1; HIFI-FRET; Job Plot; electrophoretic mobility shift assays; multi-angle light scattering; analytical ultracentrifugation; atomic force microscopy; small angle x-ray scattering

1. Introduction

The Poly (ADP-Ribose) Polymerase (PARP) family is a diverse protein family involved in many cellular processes. PARP-1, the most abundant member of this family, is implicated in the regulation of gene expression and in the DNA damage response through its ability to bind tightly to many models of DNA damage (1) as well as interact with undamaged chromatin (2, 3). In its inactive state, PARP-1 functions as a chromatin architectural protein that condenses chromatin (4). In vitro, PARP-1 binds native chromatin templates lacking

karolin.luger@colorado.edu, Phone number: 303-735-6689.

*Present Address: Van Andel Research Institute, Grand Rapids, MI

exposed DNA ends with nanomolar affinity, comparable to its affinity for various models of DNA damage (3). Upon enzymatic activation stimulated by DNA damage or other cues, PARP-1 modifies primarily itself and this affects its interaction with native chromatin much more than its interaction with free DNA ends. The ability of PARP-1 to bind native and damaged chromatin may involve different modules of the five known DNA binding domains in PARP-1 (Fig. 1A): three DNA binding zinc finger domains, a BRCA C-terminus fold (BRCT), a tryptophan-glycine-arginine (WGR) rich domain, and a catalytic domain composed of a helical domain (HD) and the ADP-ribosyl transferase (ART) domain. In its PARylated form, automodified PARP-1 gains a histone chaperone function with the ability to bind histones with low nanomolar affinity, and assemble nucleosome (3)

In this chapter, we apply various approaches to measure the interaction between PARP-1 (and truncated variants) and chromatin constructs. While we focus primarily on PARP-1, these techniques can be utilized for all three DNA-dependent Parps (Parp1-3). PARP-1 proteins were purified as previously described (5, 6), increasing the final NaCl concentration in the gel filtration buffer to 500 nM. The chromatin templates used here represent both native and ‘damaged’ chromatin. Mononucleosomes are assembled on the 601 positioning sequence at varying lengths (see (7, 8) for details on assembly and reconstitution) (Fig. 1B). The 146 base pair DNA length represents the minimal nucleosome assembly length with no DNA linker arms. 165 base pair DNA yield mononucleosomes with 7 and 11 extending base pairs; and 207 base pair has 30 base pairs of linker DNA extending symmetrically. For higher order chromatin templates, we assembled trinucleosomes on three repeats of the ‘601’ nucleosome positioning sequence (9). The non-linker ended trinucleosome (NLE-Tri) has 60 base pairs flanking the central nucleosome with no extending DNA linker ends (Fig. 1B). To distinguish interactions between free DNA and chromatin templates, trinucleosome assembly saturation is ensured via analytical ultracentriguation and restriction enzyme digestion as described (3, 10). Nuc146 and NLE-Tri represent native chromatin templates, while Nuc165 and Nuc207 represent double strand breaks in the context of chromatin.

The protocols described below allow for the quantification of the in vitro interaction of PARP-1 with chromatin in solution. We establish a protocol for fluorescently labeling PARP-1 that does not interfere with or affect automodification activity or nucleosome binding. Fluorescently labeled PARP-1, in conjunction with fluorescently labeled histones, nucleosomes, or DNA can be used to quantify apparent binding affinities and complex stoichiometries through the use of high-throughput interactions by fluorescent intensity with fluorescent resonance energy transfer (HI-FI FRET) and Job plot stoichiometry measurements (3, 5). Solution-state HI-FI FRET experiments can be complemented by electrophoretic mobility shift assays (EMSA). For solution state measurements with unlabeled substrates, multi-angle light scattering (MALS) and analytical ultracentrifugation (AUC) provide further information on PARP-1 chromatin complexes by yielding molecular weights, stoichiometries, and shape information. Lastly, atomic force microscopy (AFM) and small angle x-ray scattering (SAXS) provide low resolution shape and size information for PARP-1/chromatin constructs.

2. Materials

2.1 Automodification of PARP-1

- Activity buffer: 50 mM Tris-HCl (pH 8.0), 100 mM NaCl, 1 mM $MgCl_2$
- NAD^+ (15 mM stock in activity buffer or H_2O)
- PJ34 hydrochloride (10 mM stock in DMSO) (Sigma Aldrich)
- Standard SDS-PAGE equipment, denaturing PAGE (e.g. 8% SDS-PAGE)
- Low binding Eppendorf

2.2 Fluorescent labeling of PARP-1

- Rotating device at 4°C (e.g. Thermo Scientific Labquake™)
- Centrifuge equipped with a rotor for holding 50 mL conical tubes (e.g. Beckman Coulter Allega 21R centrifuge)
- 25 mL vivaspin concentrators (30- to 50- kDa MW cut off)
- Nanospec or any other spectrophotometer
- Standard SDS-PAGE equipment, denaturing PAGE (e.g. 15% SDS-PAGE)
- Typhoon Trio imager (GE Healthcare)
- ImageQuant TL software for visualizing
- Maleimide reactive dyes (Alexa488 or Atto-647N) in 10 mM stock in dimethyl sulfoxide (DMSO) or dimethyl fluoride (DMF); freshly made or frozen at −20°C
- Labeling Buffer: 25 mM HEPES (pH 8.0), 500 mM NaCl, 0.1 mM EDTA, 0.1 mM TCEP

2.3 Electrophoretic Mobility Shift Assay (EMSA)

- PAGE equipment at 4°C, 5% native TBE-PAGE
- Agarose gel running equipment at room temperature
- Parp Binding Buffer (PBB50 or PBB200): 25 mM Tris-HCl (pH 7.5), 50 or 200 mM NaCl, 2 mM Arginine
- Low binding Eppendorf tubes

2.4 HI-FI FRET & Job Plot

- Typhoon Trio imager (GE Healthcare)
- ImageQuant TL for visualization and quantification
- GraphPad Prism software for data analysis
- Multi-channel (12 channels) pipette (100 μL)

- 384-well black Sensoplate Plus with glass flat bottom (Greiner Bio-One International)
- 96-well block (250 or 500 μL)
- 1% (v/v) Hellmanex in H_2O
- Freshly made Sigma Cote (98% Heptane (Sigma Aldrich), 2% 1, 7 Dichlorooctamethyl-tetrasiloxane (Sigma Aldrich))
- Microplate binding buffer: 25 mM Tris-HCl (pH 7.5), 200 mM NaCl, 0.01% NP-40, 0.01% CHAPS

2.5 Size Exclusion Chromatography Multi-Angle Light Scattering (SEC-MALS)

- Wyatt Instruments HELEOS and rEX detectors outfitted with ASTRA software
- GE Healthcare HPLC
- SEC column (e.g. S200 increase 10/300 GL (24 mL) (GE Healthcare))
- PBB200 buffer: 25 mM Tris-HCl (pH 7.5), 200 mM NaCl, 2 mM Arginine, filtered through a 0.1 μm membrane
- Bovine serum albumin (BSA; 2 mg/mL (Sigma Aldrich Protein Standard))

2.6 Analytical Ultracentrifugation (AUC)

- AUC cells with quartz windows (Beckman)
- Proteome Lab XLA or XLI analytical ultracentrifuge
- Computer with Ultrascan III installed for data analysis and access to Laboratory Information Management System (LIMS) for 2 dimensional spectrum analysis (2DSA) and genetic algorithm coupled with Monte-Carlo analysis (GA-MC) calculations
- Buffer: 20 mM Tris-HCl (pH 7.5), 1 mM EDTA, 1 mM DTT, or any other buffer

2.7 Atomic Force Microscopy (AFM)

- Asylum Research MFP-3D Atomic Force Microscope or comparable instrument
- Olympus 240TS AFM tips, or comparable brand
- Freshly cleaved mica discs (SPI Supplies) glued to glass slides (VWR)
- 3-aminopropyltriethoxysilane (APTES) (Sigma Aldrich)
- Syringe filters and Syringes or Steriflips
- Sample buffer: 20 mM Tris-HCl (pH 7.5), 1 mM EDTA, 1 mM DTT, filtered through a 0.2 μm membrane

2.8 Small Angle X-ray Scattering (SAXS)

- Synchrotron beamline with SAXS data collection capabilities preferably with in-line SEC. All data in the present work was collected at Sector 18ID (BioCAT)

located at Advanced Photon Source located in Argonne National Laboratory, Chicago.

- Size exclusion column (e.g. Superose 6 or Superdex 200 (GE Healthcare))
- GE Healthcare FPLC or HPLC system
- Sample buffers: 25 mM Tris-HCl (pH 7.5), 2 mM Arginine, 50 mM NaCl and 20 mM Tris-HCl (pH 7.5), 1 mM EDTA, 1 mM DTT, filtered via 0.2 μm membrane

3. Methods

3.1 Automodification of PARP-1

PARP-1 is purified as described (6) with extra precaution taken to ensure the protein prep is free from DNA (monitor the 260/280 nm ratio closely and keep below 0.6). To study differences between unmodified and automodified PARP-1 in its chromatin interacting properties, precautions must also be taken to keep unmodified and automodified Parp reaction components the same. If done properly, any difference in interactions can be ascribed to PARylation rather than a reaction component (i.e. DNA, NAD^+, or PJ34). To accomplish this, we utilize a pre-quenched PARP-1 sample (pQ-PARP-1, quenched with PARP-1 inhibitor, PJ34, prior to the addition of activating DNA and NAD^+) as the unmodified control. To prepare automodified PARP-1, PJ34 is added after a two-hour incubation with DNA and NAD^+ (Fig. 1C). Automodification of PARP-1 (AM-PARP-1) causes a high molecular weight smear or a shifted band on a denaturing gel due to the heterogenous nature of PARylation (Fig. 1D, left panel).

1. Set up the pre-quench (pQ) PARP-1 reactions by adding 1 μM PARP-1 to activity buffer. Incubate with 1 mM PJ34 (final) for 5 minutes (See Note 1).
2. Add 100 nM DNA (53 bp DNA used here) and incubate at RT for 10 minutes followed by the addition of NAD^+ (600 μM).
3. Set up the automodification (AM) PARP-1 reaction by incubating PARP-1 (1 μM) and DNA (100 nM) for 10 minutes at RT.
4. Add 600 μM NAD^+ and incubate for 2 hours at RT. Quench reaction with 1 mM PJ34.
5. Run pre-quenched and automodification reactions on a denaturing gel (e.g. Biorad Mini-PROTEAN TGX pre-cast gel, shown here). Higher molecular weight smearing and disappearance of a single protein band on the gel is indicative of PARylation (Fig. 1D, left panel).

3.2 Fluorescent Labeling PARP-1

Here, maleimide fluorophores (such as Alexa488 or Atto-647N) are chemically conjugated to native cysteines on PARP-1. The fluorophore is added in an equimolar ratio to PARP-1 and incubated in the dark for 30 minutes. Excess fluorophore is removed through buffer

[1]The highest concentration recommended for a PARP-1 automodification reaction is 2 μM; the maximum incubation time with NAD^+ is overnight.

washes and labeling efficiency is calculated. PARP-1 can label at multiple locations (e.g. Cys-24, Cys-256, Cys-429; (5) and data not shown), so 0.1 mM TCEP in the labeling buffer can help quench the labeling process to prevent over-labeling. Mass spectrometry can be used to identify which specific residues are labeled. Once labeled, PARP-1 is run on a denaturing PAGE and stained for protein (0.5–1 μg PARP-1) (Fig. 1D, middle panel) or scanned on a phosphorimager at the appropriate wavelength to check for fluorescence (0.25–0.5 μg PARP-1; Fig. 1D, right panel). Compared to unlabeled PARP-1 samples (Fig. 1D, left panel), Alexa488 labeling (Fig. 1D, middle panel) does not affect electrophoretic mobility or automodification activity. Here, the difference in PARylation between the unlabeled and labeled PARP-1 is due to differing times of incubation (unlabeled: 1 hour; labeled: 2 hours). The automodification reaction time will influence if the PARylation modification appears as a smear or as a shifted band. Fluorescently labeled PARP-1 can be used in FRET binding assays and Job plot stoichiometry measurements as described in the next section.

1. Add equimolar (1 to 1) ratio of fluorophore to protein in a low binding Eppendorf tube (See Note 2).
2. Wrap the tube in aluminum foil and rotate in the dark at 4°C for 15 minutes.
3. Add labeled protein to a 15 mL falcon concentrator (e.g. 50 kDa MW cutoff for PARP-1).
4. Add 1–2 mL of labeling buffer for each buffer exchange (See Notes 3 and 4).
5. Spin concentrator at 4000 k for 10–15 min.
6. Repeat steps 4 and 5 until flow through is colorless to the eye. Then repeat 1–`2 more times.
7. Determine the concentration of the protein and dye by absorbance. Labeling efficiency is calculated by determining the ratio of dye molarity to protein molarity (See Note 5).
8. Analyze 0.25–0.5 μg of the labeled protein on a 15% SDS-PAGE (or other denaturing PAGE). Scan gel at the Typhoon at the proper wavelength to confirm fluorescent labeling, then stain for protein. Increase sample size to 1 μg for protein stain (or alternately use a sensitive method of protein detection like silver stain) if checking for degradation or staining automodified PARP-1 reactions (Fig. 1D).
9. Flash freeze in 5–10 μL aliquots in liquid nitrogen and store at −80°C (See Note 6).

[2]For labeling buffer, use the buffer the protein was last in – typically the gel filtration buffer. Protein concentration for labeling can range from 20–100 μM.
[3]Other Parp family members such as PARP-2 label more efficiently with Oregon Green 488 iodoacetamide, not Alexa488 maleimide, for donor fluorophore. You may need to try various fluorophores.
[4]Always add fresh reducing agent such as pH-adjusted TCEP (not DTT), to the labeling buffer.
[5]We typically achieve 50–80% labeling efficiency. If over-labeling (100% or more) occurs, continue with buffer washes or run sample over a PD10 column, then decrease fluorophore concentration and/or incubation time for future labeling experiments.
[6]Thaw each aliquot once and use within 1–2 days.

3.3 Electrophoretic Mobility Shift Assay (EMSA)

For a qualitative approach to Parp complex formation with DNA and/or nucleosomes, electrophoretic mobility shift assays are performed (3, 11). Purified Parp proteins (e.g. PARP-1 or N-Parp) are titrated against reconstituted mono- or trinucleosomes and incubated overnightat 4°C. Mononucleosome complexes are analyzed by native PAGE and stained for DNA and protein (Fig. 1E). Fluorescently labeling PARP-1 and nucleosomes (647-Nuc165, Fig. 1E, lanes 7– 10) does not affect their respective mobility or complex formation when compared to unlabeled reagents (Fig. 1E, lanes 3–6). Trinucleosome-Parp complexes are run on a 1% agarose gel and also stained for DNA with Ethidium Bromide and protein with Imperial protein stain (Fig. 1F). Although in theory, binding constants can be derived from this approach, this technique is not accurate and other more quantitative approaches are needed. However, analysis of material prior and after analysis by any of the other approaches listed below will yield valuable verification that indeed complex formation was being measured.

1. Mononucleosomes or DNA are titrated with increasing molar ratios of PARP-1 (or PARP-1 mutant proteins) in PBB50 or PBB200 (See Notes 7–8).
2. Reactions are incubated overnight at 4°C.
3. 5 μL aliquot of the reaction mix is analyzed on a 5% (w/v) native TBE-PAGE at 4°C at 150 V for 60 min. for mononucleosomes and DNA. For trinucleosome complexes, see Note 9.
4. Gels are stained with ethidium bromide followed by Imperial protein stain to visualize for DNA and protein respectively (Fig. 1E and 1F).

3.4 HI-FI FRET Binding Assay & Job Plot Stoichiometry Measurement

High-throughput interactions by fluorescent intensity with fluorescent resonance energytransfer (HI-FI FRET) provides a highly sensitive and in solution assay for measuring apparentbinding affinities of Parp with a variety of substrates (e.g. mononucleosomes, trinucleosomes, DNA) (3, 5, 12, 13). The assay is schematically represented in Fig. 2A, top panel. Here, acceptorlabeled ligand (e.g. Nuc165; Fig. 2A, bottom panel) is titrated from 0 nM to 1000 nM. Donorlabeled Parp (e.g. PARP-1; Fig. 2B, bottom panel) is held constant at low nanomolarconcentrations. If a binding event occurs, the donor fluorophore will be within Forster distanceof the acceptor fluorophore and thus energy transfer can occur (i.e. a FRET signal is observed).The FRET signal can be mathematically corrected to quantify apparent binding affinities. Forexample, PARP-1 binds nucleosomes with linker arms (Nuc165) with low nanomolar affinity, while nucleosomes with no linker arms, such as Nuc146, exhibit weak (> 500 nM) affinity andno saturatable plateau (Fig. 2B) (also seen with Sf9 expressed PARP-1, (3, 5)).

---

[7]The arginine in the binding buffer is optional and doesn't affect the mobility shift.
[8]Complexes are typically set up at ~1–1.5 μM nucleosome; PARP-1 or N-Parp are titrated between 0.6–1.2 excess over the nucleosome.
[9]Trinucleosomes and their complexes are analyzed on a 1% agarose gel in 1× TAE buffer at 50 V for 2 hours at room temperature. Gels were stained as described.

To study the effect of PARP-1 automodification on its interactions with various substrates, pre-quenched and automodified PARP-1 probes were prepared (Fig. 1C). The pre-quenched and automodified PARP-1 probes both contain low nanomolar amounts of DNA as well as excess NAD^+ and PJ34 in each sample. Comparing the pre-quenched to PARP-1 reactions to PARP-1 without these components proved that these additional reaction components do not affect the apparent K_D (3). However, PARylation weakens PARP-1 binding to NLE-Tri by a factor of 20 (Fig. 2D) (3).

HIFI-FRET can be paired with Job plot continuous variation measurements to elucidate the stoichiometries ((14), and applied to PARP-1 in (3)). Here, the amount of donor labeled PARP-1 is increased in incremental titration steps while the acceptor labeled ligand (e.g. Nuc165 or dsDNA) is decreased in similar steps (see schematic in Fig. 2D, top panel). This process keeps the overall molar ratio equal to 1 and therefore, the peak of the analyzed curve will yield the ideal (peak) molar ratio (Parp:Nuc165 or Parp:DNA). In this example, a titration of PARP-1 against Nuc165 yields a peak at 0.5, indicating a stoichiometry of one PARP-1 molecule per mononucleosome (Fig. 2C, black curve). PARP-1 binds DNA in a 2 to 1 ratio indicated by the peak at 0.66 (0.66 PARP-1 per 0.33 DNA) (Fig. 2C, gray curve). Job plots quantitatively identify a variety of stoichiometries ranging from 1 to 1 (n to n), 2 to 1, or 1 to 2, etc. A caveat of Job plot is that a peak at a 0.5 molar ratio is consistent with 1:1 or 2:2 (or n:n) stoichiometry, and hence other methods are needed to distinguish between these possibilities. Thus, results should be verified by SEC-MALS or AUC. These two approaches also reveal any problems with homogeneity and mono-dispersity of any given complex.

3.4.1 HIFI-FRET Microplate Treatment

1. Fill each well of the 384-well plate with 1% Hellmanex and incubate for 15–20 min.
2. Rinse the plate thoroughly with distilled water. Repeat rinses 4×.
3. Let plate dry overnight.
4. Fill each well with freshly made homemade sigma cote in a well ventilated hood.
5. Once each well is filled, rinse plate 4× with distilled water.
6. Let plate dry overnight. Treated microplates can be stored for 2–3 months in bubble wrap to prevent dust from getting into the wells.

3.4.2 HIFI-FRET Plate Set Up

1. Clean the glass of the microplate with H_2O, then 100% EtOH, followed by H_2O again, wipe dry using lint-free kimwipes.
2. In a 96-well plate, label two rows 1–23 (odd numbers in row A and even numbers in row B).
3. Ligand titration series are set up at a concentration 2× the final concentration. Final titration concentration depends on the K_D (See Note 10).

[10]The titration series should have a final concentration ~10–20-fold greater than the expected K_D.

4. Serially diluted master stock concentrations are set up (ex: 1000 nM, 500 nM, 100 nM).

5. Ligand titration set up by adding buffer to each well followed by ligand and mixing thoroughly. The first two titration points should always be buffer-only (0 nM ligand).

6. Parp probe concentrations are decided based on the apparent K_D. If the apparent K_D is not 5× below [P], you cannot rely on the single site binding equation which assumes P exists in two states: free and bound. If [P] ≥ K_D, all of the probe will be bound (FB = 100) and therefore, the assumption is false. In these cases, the quadratic equation with two or three probe concentrations must be used to eliminate this assumption. See Equation 1 and Note 11.

$$P + L \leftrightharpoons \mathrm{PL} \quad \text{Equation 1}$$

7. Probe concentrations are set up 2× the final concentration and at a volume of 1500 μL.

8. 20 μL of the acceptor titration is set up in duplicate for acceptor only and each FRET series. 20 μL of microplate binding buffer is added to the acceptor only lanes. Each Parp probe (20 μL) is then added in duplicate to each FRET series. The total volume in each well is 40 μL.

3.4.3 HIFI-FRET Automodification Binding Plate Set Up

1. Repeat steps 1–8 for the unmodified binding assay set up with a minor change: for automodified binding assays, two types of probes will be set up, a pre-quench probe and an automodified probe (see schematic for reaction set up in Fig. 1C and protocol for automodified PARP). Again, probe concentrations will depend on apparent K_D, as discussed above.

3.4.4 HIFI-FRET Plate Scanning

1. Clean typhoon glass with 70% EtOH followed by H_2O

2. Scan the plate at 200 μm with +3 mm plane at the following wavelengths and voltages (See Note 12).

   - Acceptor Channel (A): Ex/Em: 633/670 nm; PMT: 400 V
   - Donor Channel (D): Ex/Em: 488/520 nm; PMT: 420 V
   - FRET Channel (F): Ex/Em: 488/670 nm; PMT: 500 V

3. See Notes 13 and 14 for further details on scanning and qualitative analysis of the plate. See sample plate scan in Fig. 2A, bottom panel.

[11] Single Site ex: PARP-1 + Nuc146; Quadratic ex: PARP-1 + Nuc165. To start, probe concentrations should be around 2–3 nM. Probe concentrations can be increased based on signal and expected K_D.

[12] PMT values can be increased or decreased based on the concentration of the ligand and probes, or labeling efficiency.

3.4.5 HIFI-FRET Data Analysis

1. Open scans (.ds file) from typhoon in ImageQuant TL.
2. Use the array analysis to quantify each well in the plate. Use the buffer-only wells as a background (negative) control.
3. Export the data from the acceptor, donor, and FRET channels to Microsoft Excel.
4. Calculate the direct excitation by the acceptor (χ_A) by using Equation 2.1. Average the direct excitation values for each titration point.
5. Calculate the donor bleed through (χ_D) by using Equation 2.2. The first two wells in each FRET series are donor only controls (0 nM ligand). Average the donor bleed through (4 values) per probe used.

$$2.1\ \chi_A = (F \div A)_{\text{Acceptor only } (L)} \qquad 2.2\ \chi_D = (F \div A)_{\text{Donor only } (P)} \quad \text{Equation 2}$$

6. Calculate the FRET corrected ($FRET_{corr}$) by using Equation 3. The direct excitation value (χ_A) must correspond to each titration point, while the donor bleed through (χ_D) is a single number per probe used. $F^{\#}$, $A^{\#}$, and $D^{\#}$ are values for the FRET series (P+L).

$$\text{FRET}_{\text{corr}} = [F^{\#} - (\chi_A \times A^{\#}) - (\chi_A \times D^{\#})] \quad \text{Equation 3}$$

7. Graph the FRET corrected values in GraphPad Prism using the ligand titration series as X-axis values and FRET corrected on Y-axis.
8. If the probe concentration, [P], is 5× below the K_D, analyze the data with the single site binding equation (Equation 4). If the probe concentration is less than 5× below the K_D and multiple probe concentrations were used, analyze the data with the quadratic equation to yield a global K_D (Equation 5). Use the numerical value of probe concentration (e.g. '5' for a 5 nM probe) to label each Y-column. See Note 15 for further details on data analysis.

$$\text{FRET}_{\text{corr}} = (Y_{\max} - Y_{\min}) \times \text{FB} + Y_{\min} \qquad \text{FB} = \frac{[L]_{\text{Total}}}{([L]_{\text{Total}} + K_D)} \quad \text{Equation 4}$$

[13] If splotches or swirls appear in the well, the protein and ligand may have aggregated. In this case, buffer conditions may need to be re-optimized or plates will need to be freshly treated.

[14] Speckles can occur in automodified Parp samples, but should not affect data analysis and resulting apparent K_D. Speckles can be eliminated by spinning the sample at 10k rpm for 10 minutes prior to adding probe to the microplate.

[15] The binding curve must reach an upper plateau to obtain reliable binding constants. Likewise, the beginning of the binding curve needs to exhibit a baseline.

$$FB = \frac{([P]+[L]_{Total}+K_D) - \sqrt{([P]+[L]_{Total}+K_D)^2 - 4[P][L]_{Total}}}{2[L]_{Total}} \quad \text{Equation 5}$$

3.4.6 Job Plot Plate Set Up

1. Clean the bottom of the microplate glass with H_2O, followed by EtOH, followed again by H_2O, wipe dry with using lint-free kimwipes.
2. Dilute the donor labeled PARP-1 and acceptor labeled ligand (nucleosomes or DNA) into a master stock that is 2× the final concentration (e.g. 2000 nM master stock for a 1000 nM titration series).
3. Set up two titration series. First, in the donor labeled Parp series, Parp will increase in incremental steps (e.g. 25 nM). Second, the acceptor labeled ligand (nucleosomes or DNA) will decrease in the same incremental step (See Note 16).
4. In duplicate, add 20 μL acceptor (ex: Nuc165) titration series followed by 20 μL donor (ex: PARP-1) titration series to the treated microplate.
5. Add a buffer-only (40 μL buffer), acceptor only (20 μL acceptor + 20μL buffer), donor only (20 μL donor + 20 μL buffer) to the plate in duplicate. The buffer-only control serves as background correction, the acceptor only will yield an averaged single direct excitation value, and the donor only will yield an averaged single donor bleed through value.

3.4.7 Job Plot Plate Scanning

1. Scan according to HIFI-FRET scanning protocol described above.

3.4.8 Job Plot Data Analysis

1. Follow steps 1–6 for HIFI-FRET plate quantification in ImageQuant TL and use equations 2.1, 2.2, and 3 to calculate FRET corrected (See Note 17).
2. Plot FRET corrected (Y-values) against the molar ratio (X-values).
3. The peak of the curve indicates the ideal molar ratio of Parp (χ_P) (See Note 18).
4. In the case of DNA, the peak is 0.66. To calculate the stoichiometry, divide 0.66 Parp by 0.33 DNA to yield 2 PARP-1 to 1 DNA molecule. In the case of Nuc165, the peak is 0.5 to yield a 1 to 1 ratio of PARP-1 per mononucleosome (See Notes 19 and 20).

[16]Increasing the donor and decreasing the acceptor in identical incremental steps maintains the overall molar ratio (protein to ligand) equal to 1.
[17]Instead of a titration series of acceptor only (acceptor + buffer), here there will only be 1 value averaged from the two acceptor only wells.
[18]Equation 6.1 (PL) would yield a peak at 0.5; P_2L (Equation 6.2) would yield a peak at 0.66; PL_2 (Equation 6.3) would yield a peak at 0.33.
[19]If the ideal molar ratio doesn't equal a whole number, multiply the entire stoichiometry to yield a whole number. Ex: 0.33 peak would yield 0.5 Parp to 1 ligand. Multiplying the stoichiometry by two would yield 1 Parp to 2 ligand (PL_2).

$$6.1\ P+L \leftrightharpoons \mathrm{PL} \qquad 6.2\ 2P+L \leftrightharpoons P_2L \qquad 6.3\ P+2L \leftrightharpoons \mathrm{PL}_2$$

Equation 6

$$\chi_P=\frac{[P]}{([P]+[L])}=1-\chi_L$$ Equation 7

$$\mathrm{Stoichiometry}=\frac{\chi_P}{(1-\chi_P)}$$ Equation 8

3.5 Size Exclusion Chromatography with Multi Angle Light Scattering (SEC-MALS)

Size exclusion chromatography coupled with multi-angle light scattering uses laser light scattering to provide information about shape and size of pre-fractionated protein samples in solution. Here, this method can be used to determine homogeneity, molecular weight, and stoichiometry of various complexes (e.g. PARP-1 in complex with the mononucleosome). Coupling MALS with SEC allows for species separation in solution as the species are eluted separately off the column. However, one caveat with this method is that smaller than two-fold differences in molecular weight cannot be detected (in these cases, AUC, described below, would be a more appropriate method). In order to perform SEC-MALS experiments, a HPLC system needs to run a suitable size exclusion column connected to a MALS and refractive index (RI) detector. Here, we analyze PARP-1 interactions with a mononucleosome assembled on 207 base pair DNA (Nuc207; Fig. 3A) (5). PARP-1 and the nucleosome alone give rise to molecular weights within error of the theoretical molecular weight. Combining equimolar amounts PARP-1 and Nuc207 yields a shift in elution, and a molecular weight within 0.3% of the theoretical molecular weight of a 1:1 complex (Fig. 3A, Table). Adding excess PARP-1 yields a free PARP-1 peak and no further shift of the complex peak illustrating the stoichiometry of PARP-1 for Nuc207 remains 1 to 1 (Fig. 3A, Table).

1. Prepare 120 μL of nucleosome solution at about 0.2–0.5 mg/ml and 120 μL of Parp alone solution at ~2 mg/mL (use higher concentrations for smaller proteins) (See Notes 21 and 22).
2. Incubate desired titrations of Parp with nucleosome or DNA overnight in 120 μL at 4°C.

[20] Unstable reducing agents such as DTT or BME, or other unstable buffer components such as detergents should be avoided. pH-adjusted TCEP should be used as the reducing agent.
[21] Thoroughly dialyze or buffer exchange samples in the running buffer to avoid high background due to buffer differences.
[22] It is recommended that a BSA standard (2 mg/mL) be run as a control prior to testing samples.

3. Equilibrate the column with buffer pre-filtered through a 0.1 μm membrane (See Note 23).

4. Spin the sample at 14,000 rpm for 10 minutes and inject 100 μL into the SEC column with a micro-syringe. Alternately a micro-filtration centrifugal device can be used.

5. Unicorn software is used to run the SEC, while the ASTRA software from Wyatt records the MALS and RI data. Refer to the manufacturer manual for details.

3.6 Analytical Ultracentrifugation (AUC)

Sedimentation velocity is used to analyze particles in solution based on rate of sedimentation. The analysis of sedimentation rates provides information on the size and shape of the particle. Data collection should be collected in intensity mode rather than absorbance to minimize noise levels (15). For further details on AUC methodology and set up, see (7). Importantly, chromatin of various sizes (mono-, tri- or arrays) or Parp proteins (e.g. PARP-1 or N-Parp) can be analyzed on their own or in combination. Here, we demonstrate that PARP-1 and N-Parp (1–486) proteins are homogeneous species with S_{avg} ($S_{20,w}$) values of 5S and 3.2S, respectively (Fig. 3B). Upon addition of mononucleosome (Nuc165, S_{avg}, 12S), S values shift to S_{avg} 14S and 13S, respectively (Fig. 3C). The shift of the mid-point S value confirms complex formation, while the homogenous shift indicates a single population and single binding event. A similar phenomenon is also seen with NLE-Tri (S_{avg} 17S) in complex with N-Parp (S_{avg} 21S) (Fig. 3D), although trinucleosomes and trinucleosome/Parp complexes are more heterogeneous due to the flexible nature the connecting linker DNA.

1. Clean AUC cell components and assemble the cell (See Ref. (7) for more detail and clarification).

2. For Parps, nucleosomes, and complexes, ~0.3–0.4 sample absorbance (at 260 or 280 nm) in 400 μL volume is required for high-quality data. Dilute sample in sample buffer (See Note 24).

3. Prepare sample (for example, mono or tri-nucleosomes) in the final dialysis buffer or the binding buffer and collect data in intensity mode. Use water in reference channels.

4. Rotor speed needs to be calibrated based on size of the particles in the sample. The smaller size of the particle, the higher the speed needed to sediment it fully. For example, mononucleosome samples (~220 kDa) should be spun at 40k rpm while 30k rpm should be used for trinucleosome samples (~650 kDa).

5. Data collection is dependent upon the number of scans representing the full spectrum of sample sedimentation (from the top to the bottom of the cell). The

[23]Resolution power and lack of contaminations on the SEC column are essential to minimize light scattering background signal. Refer to the manufacturer's instruction for cleaning procedures. Leaching of particles from column results in an unstable baseline.
[24]Any buffer is compatible with AUC, but DTT above 1 mM should be avoided. BME and detergents should also be avoided due to background scatter.

number of scans depends on the molecular weight of the samples, the speed of the rotor, the number of samples in the rotor, etc. (See Note 25).

6. AUC data analysis is performed using the Ultrascan 3 software by following the user manual details found here: http://www.ultrascan2.uthscsa.edu/manual2/index.html (16–19).

3.7 Atomic Force Microscopy (AFM)

Atomic force microscopy allows for low-resolution visualization of complexes, in addition to providing estimates of volume and height. The measurement is based on the capacity of the sample to reflect laser light off a cantilever during surface scanning. Here we describe AFM data collection in air to allow for rapid direct visualization of complexes, e.g. PARP-1 in complex with trinucleosomes (Fig. 4) (3). The approach is particularly powerful if used with defined nucleosomal arrays (7, 20, 21). In this case, the 1×1 μm scan images obtained with NLE-Tri indicates three nucleosomes held together by linker arms with a height profile of ~1.5–2 nm (Fig. 4A). The addition of PARP-1 shows compaction of the NLE-Tri as indicated by a height profile increase to 3–5 nm (Fig. 4B). This compaction is alleviated when PARP-1 is automodified, as the height profiles return to 1.5–2 nm (Fig. 4C).

2.7.1 Procedure

1. Use scotch tape to cleave mica. Press tape down on the mica disc and peel off repeatedly to ensure that a smooth mica surface is obtained. Modify freshly cleaved mica with APTES by adding 30 μL of a 1 in 1000 dilution in water onto the mica disc. Incubate the covered disc for 30 minutes at room temperature. Rinse the disc with 0.2 μm filtered water and gently dry using a pure nitrogen stream.

2. Dilute the sample using sample buffer. For example, trinucleosome samples are diluted to ~1.5 ng/μL but dilution range depends on sample.

3. Pipette 30 μL of the diluted sample onto the APTES-mica disc and let stand for 5–15 min.

4. Rinse the disc surface with sample buffer, and gently dry with pure nitrogen or compressed air.

5. Wipe off any residual buffer droplets from the sample area and place the slide on the microscope stage. Secure the stage with magnets.

6. Begin scanning the sample area with 5 × 5 μm areas. Once well-spread areas are identified, narrow the scope to 2 × 2 μm scans. Increase resolution to 1 ×1 μm scans and continue to increase resolution if the instrument is capable. However, at higher resolution scans (i.e. smaller areas), the noise will increase due to the high sensitivity.

[25]Generally, 150 scans should be collected per sample.

2.7.2 AFM Data Processing

1. Images from the data collection are 'flattened' and analyzed using MFP-3D software (Asylum) or a comparable software.
2. Each 1×1 μm image in Fig. 4 was divided into four quadrants and zoomed in digitally to obtain a clear view trinucleosomes.
3. Multiple free hand lines were drawn through the particles to obtain height profiles (Fig. 4; insets on right side) For statistical analysis, a large number of images should be analyzed (See Note 26).

3.8 Small Angle X-Ray Scattering (SAXS)

Small angle x-ray scattering is used to obtain low resolution size and shape information on individual proteins or protein complexes. Data is collected at a synchrotron equipped with SAXS beamlines (e.g. APS Chicago – BioCAT, Sector 18ID). SAXS data collection should ideally be coupled with size exclusion chromatography (SEC-SAXS) (22). The addition of SEC separates any free chromatin components from the sample prior to SAXS data collection. We need to have a q-range suitable for larger macromolecules such as the mono- and trinucleosome complexes. The approximate q_{min} required to study any given macromolecule is considered to be π/D_{max}. Here, we show SEC-SAXS analysis of radiation of gyration (R_g) and maximum dimension (D_{max}) for the mononucleosome and the nucleosome in complex with N-Parp (Fig. 5). The data indicates the mononucleosome alone yields a spherical envelope (R_g: 47Å; D_{max} 157Å) (Fig. 5B) (23, 24). The N-Parp and mononucleosome complex shows an increase in dimension; however, while the R_g and D_{max} values are not additive, the values are larger than the nucleosome indicative of binding (R_g: 55Å; D_{max} 194Å) (Fig. 5C and D).

1. Write a proposal requesting beam time. Proposal submission procedures and deadlines can be found on beamline web sites.
2. Concentrate individual samples (e.g. N-Parp and Nuc165) to ~2 mg/mL in ~150 μL in low binding Eppendorf tubes. Save an aliquot pre- and post-concentration for examining the complexes by other methods (such as EMSA and AUC, see above).
3. Samples must be prepared and shipped to the beamline a day or two in advance. For Parp samples, ship on dry ice to maintain −80°C. Chromatin samples should not be frozen. Instead, make an ice pack by filling Ziploc bags with ice and place samples sealed in 50 mL falcon tubes inside.
4. Arrive at the beamline the night before for wet lab set up, such as preparation of buffers and any complexes (e.g. N-Parp + mononucleosomes). Set up Parp complexes as described above.
5. Complete SAXS data collection for individual components as well as complexes (See Notes 27 and 28).

[26]Microsoft Excel can be used to analyze results for easy visualization and comparison of images.

6. Clean the quartz sample chamber after each run using a Hamilton Syringe Pump sequentially with water, bleach, water, isopropanol, and water to prevent cross contamination between runs.

7. Data-reduction (radial averaging of the scattering intensities to generate I (q) vs q plots), usually involves software indigenous to the beam line and should be done at the beamline. Subtract buffer from sample data.

8. All further data processing can be done with the ATSAS suite. R_g and D_{max} can be determined by Primus in ATSAS (25).

9. Ab initio modelling is done using Dammin (26).

10. Images of the envelopes can be generated in VMD by first generating a shell in pdb2vol (27–29).

References

1. Langelier MF, Riccio AA, Pascal JM. PARP-2 and PARP-3 are selectively activated by 5' phosphorylated DNA breaks through an allosteric regulatory mechanism shared with PARP-1. Nuc Acids Res. 2014; 42:7762–75. DOI: 10.1093/nar/gku474
2. Kraus WL. Transcriptional control by PARP-1: chromatin modulation, enhancerbinding, coregulation, and insulation. Curr Opin Cell Biol. 2008; 20:294–302. DOI: 10.1016/j.ceb.2008.03.006 [PubMed: 18450439]
3. Muthurajan UM, Hepler MRD, Hieb AR, et al. Automodification switches PARP-1 function from chromatin architectural protein to histone chaperone. PNAS. 2014; 111:12752–12757. [PubMed: 25136112]
4. Wacker DA, Ruhl DD, Balagamwala EH, et al. The DNA binding and catalytic domains of poly(ADP-ribose) polymerase 1 cooperate in the regulation of chromatin structure and transcription. Mol Cell Biol. 2007; 27:7475–85. DOI: 10.1128/MCB.01314-07 [PubMed: 17785446]
5. Clark NJ, Kramer M, Muthurajan UM, Luger K. Alternative modes of binding of poly(ADP-ribose) polymerase 1 to free DNA and nucleosomes. J Biol Chem. 2012; 287:32430–9. DOI: 10.1074/jbc.M112.397067 [PubMed: 22854955]
6. Langelier MF, Planck JL, Servent KM, Pascal JM. Purification of human PARP-1 and PARP-1 domains from Escherichia coli for structural and biochemical analysis. Methods Mol Biol. 2011; 780:209–26. DOI: 10.1007/978-1-61779-270-0_13 [PubMed: 21870263]
7. Muthurajan U, Mattiroli F, Bergeron S, et al. In Vitro Chromatin Assembly: Strategies and Quality Control. Methods Enzymol. 2016
8. Dyer PN, Edayathumangalam RS, White CL, et al. Reconstitution of Nucleosome Core Particles from Recombinant Histones and DNA. Methods Enzym. 2004; 375:23–44.
9. Lowary PT, Widom J. New DNA sequence rules for high affinity binding to histone octamer and sequence-directed nucleosome positioning. J Mol Biol. 1998; 276:19–42. DOI: 10.1006/jmbi.1997.1494 [PubMed: 9514715]
10. Winkler DD, Muthurajan UM, Hieb AR, Luger K. Histone chaperone FACT coordinates nucleosome interaction through multiple synergistic binding events. J Biol Chem. 2011; 286:41883–92. DOI: 10.1074/jbc.M111.301465 [PubMed: 21969370]

[27] Inline SEC-SAXS is better for collecting data collection on chromatin because it allows for fractionation and removal of unbound components prior to SAXS data collection. Even though the samples undergo dilution, it is still possible to calculate the exact concentration if the scattering plots and the UV chromatogram are synchronized.

[28] It is important to keep track of sample amounts loaded onto SEC, and to compare it with the relative UV signal of the eluate to determine if any aggregates were retained in the column.

11. Hellman LM, Fried MG. Electrophoretic mobility shift assay (EMSA) for detecting protein-nucleic acid interactions. Nat Protoc. 2007; 2:1849–1861. DOI: 10.1038/nprot.2007.249 [PubMed: 17703195]
12. Hieb AR, D'Arcy S, Kramer MA, et al. Fluorescence strategies for high-throughput quantification of protein interactions. Nuc Acids Res. 2012; 40:e33.doi: 10.1093/nar/gkr1045
13. Winkler DD, Luger K, Hieb AR. Quantifying chromatin-associated interactions: the HI-FI system. Methods Enzymol. 2012; 512:243–274. DOI: 10.1016/B978-0-12-391940-3.00011-1 [PubMed: 22910210]
14. Olson EJ, Buhlmann P. Getting more out of a Job plot: determination of reactant to product stoichiometry in cases of displacement reactions and n:n complex formation. J Org Chem. 2011; 76:8406–12. DOI: 10.1021/jo201624p [PubMed: 21895009]
15. Kar SR, Kingsbury JS, Lewis MS, et al. Analysis of Transport Experiments Using Pseudo-Absorbance Data. Anal Biochem. 2000; 285:135–142. DOI: 10.1006/abio.2000.4748 [PubMed: 10998273]
16. Cao W, Demeler B. Modeling analytical ultracentrifugation experiments with an adaptive space-time finite element solution of the Lamm equation. Biophys J. 2005; 89:1589–1602. DOI: 10.1529/biophysj.105.061135 [PubMed: 15980162]
17. Brookes E, Demeler B. Genetic Algorithm Optimization for Obtaining Accurate Molecular Weight Distributions from Sedimentation Velocity Experiments. Prog Colloid Polym Sci. 2006; 131:33–40.
18. Demeler, B. UltraScan - A Comprehensive Data Analysis Software Package for Analytical Ultracentrifugation Experiments. In: Scott, DJ.Harding, SE., Rowe, AJ., editors. Mod. Anal. Ultracentrifugation Tech. Methods. Royal Society of Chemistry (UK); 2005. p. 210-229.
19. Demeler B, van Holde KE. Sedimentation velocity analysis of highly heterogeneous systems. Anal Biochem. 2004; 335:279–288. DOI: 10.1016/j.ab.2004.08.039 [PubMed: 15556567]
20. Rogge RA, Kalashnikova AA, Muthurajan UM, et al. Assembly of nucleosomal arrays from recombinant core histones and nucleosome positioning DNA. J Vis Exp JoVE. 2013; doi: 10.3791/50354
21. Muthurajan UM, McBryant SJ, Lu X, et al. The linker region of macroH2A promotes self-association of nucleosomal arrays. J Biol Chem. 2011; 286:23852–23864. DOI: 10.1074/jbc.M111.244871 [PubMed: 21532035]
22. Lambright D, Malaby AW, Kathuria SV, et al. Complementary techniques enhance the quality and scope of information obtained from SAXS. Trans. Am. Crystallogr. Assoc. Annu. Meet. 2013
23. Dechassa ML, Wyns K, Li M, et al. Structure and Scm3-mediated assembly of budding yeast centromeric nucleosomes. Nat Commun. 2011; 2:313.doi: 10.1038/ncomms1320 [PubMed: 21587230]
24. Yang C, van der Woerd MJ, Muthurajan UM, et al. Biophysical analysis and smallangle X-ray scattering-derived structures of MeCP2-nucleosome complexes. Nucleic Acids Res. 2011; 39:4122–4135. DOI: 10.1093/nar/gkr005 [PubMed: 21278419]
25. Petoukhov MV, Franke D, Shkumatov AV, et al. New developments in the ATSAS program package for small-angle scattering data analysis. J Appl Crystallogr. 2012; 45:342–350. DOI: 10.1107/S0021889812007662 [PubMed: 25484842]
26. Svergun DI. Restoring low resolution structure of biological macromolecules from solution scattering using simulated annealing. Biophys J. 1999; 76:2879–2886. DOI: 10.1016/S0006-3495(99)77443-6 [PubMed: 10354416]
27. Humphrey W, Dalke A, Schulten K. VMD: visual molecular dynamics. J Mol Graph. 1996; 14:33–38. 27–28. [PubMed: 8744570]
28. Wriggers W, Milligan RA, McCammon JA. Situs: A package for docking crystal structures into low-resolution maps from electron microscopy. J Struct Biol. 1999; 125:185–195. DOI: 10.1006/jsbi.1998.4080 [PubMed: 10222274]
29. Wriggers W, Chacon P. Using Situs for the registration of protein structures with low-resolution bead models from X-ray solution scattering. J Appl Crystallogr. 2001; 34:773–776. DOI: 10.1107/S0021889801012869

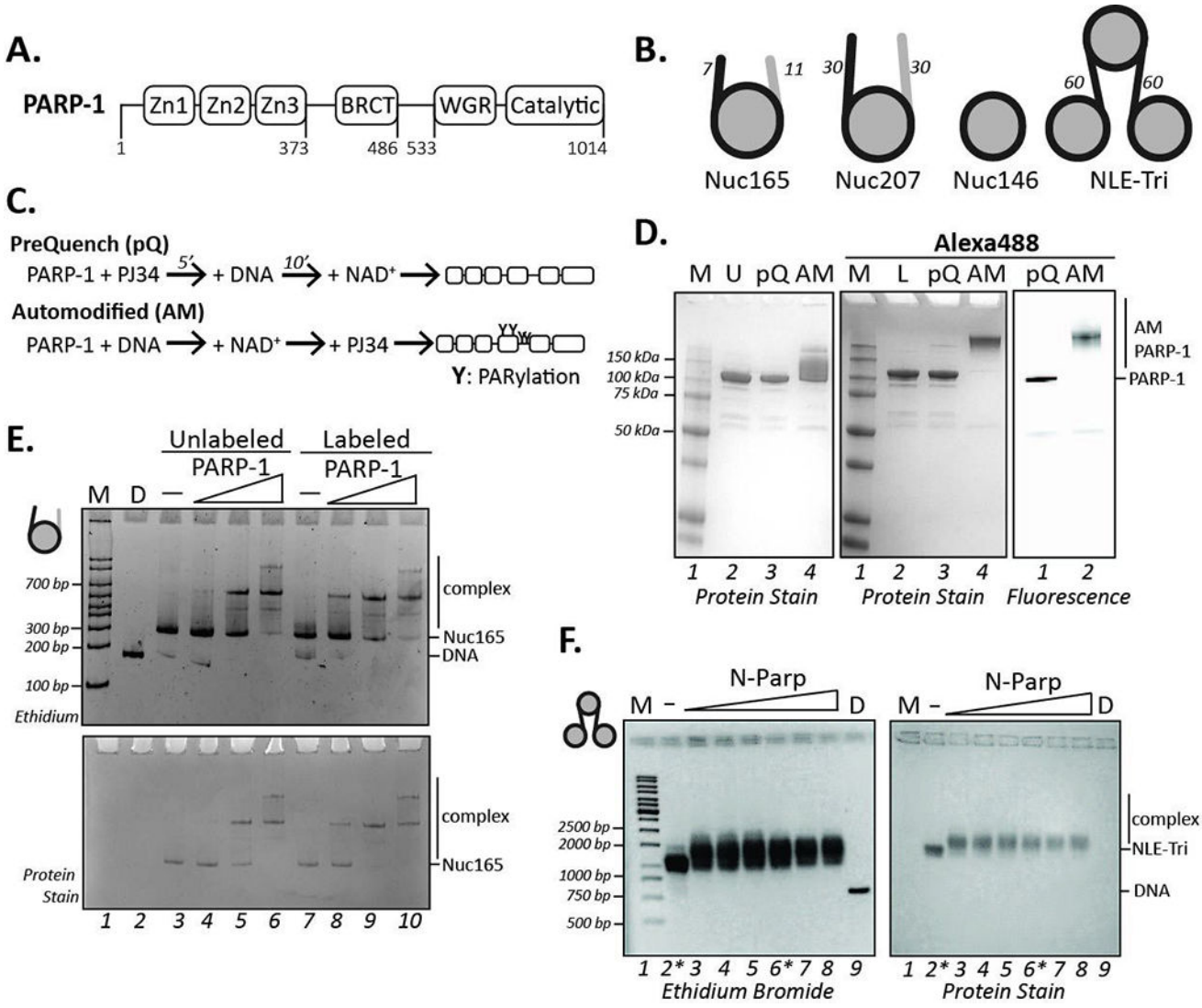

Figure 1. PARP-1 – chromatin interactions analyzed by native PAGE

A. PARP-1 is a multi-domain protein. The N-Parp construct used here is composed of residues 1–486.

B. Schematic of mononucleosomes and trinucleosomes used in assays discussed here. Nuc146 and NLE-Tri do not have exposed DNA linker ends, while Nuc165 and Nuc207 do.

C. Schematic for preparing automodified and ‘mock-automodified’ PARP-1. Pre-quenching with a Parp inhibitor (PJ34) prior to addition of DNA and NAD^+ inhibits the NAD^+ binding site in PARP-1. Automodified PARP-1 samples are quenched with PJ34 after incubation with DNA and NAD^+. Each probe has the same reaction components to ensure binding affinity differences are due to PARylation.

D. PAGE analysis of Alexa-488 fluorescently labeled PARP-1. PARP-1, pre-quenched PARP-1 (pQ), and automodified PARP-1 (AM) were run on a denaturing PAGE. Left: Protein stain of 1 μg unlabeled PARP-1 reactions. Lane 1, molecular weight marker; Lane 2, PARP-1 alone; Lane 3, pre-quenched PARP-1; Lane 4, automodified PARP-1. Middle: Protein stain of 1 μg Alexa488 labeled PARP-1. Lane 1, molecular weight marker; Lane 2,

PARP-1 alone; Lane 3, pre-quenched PARP-1; Lane 4, automodified PARP-1. Right: Cy2 (ex/em: 473/520 nm) typhoon scan of 0.25 μg Alexa488 labeled PARP-1. Lane 1, pre-quenched PARP-1; Lane 2, automodified PARP-2; Lane 3, molecular weight marker. Both unlabeled and labeled PARP-1 samples show a single homogenous band (with less than 5% degradation), while automodification (AM) creates a heterogeneous smear or shifted band on the gel due to PARylation.

E. EMSA analysis of PARP-1, unlabeled and Alexa488 labeled, with unlabeled and Atto-547N labeled mononucleosomes. Nuc165 was incubated with PARP-1 (0.5, 1, and 1.5-fold excess) and analyzed on a 5% TBE-PAGE. Gels were stained as indicated. FL-PARP-1 binding to mononucleosomes results in a supershifted band. Addition of a fluorescent label to PARP-1 and Nuc165 does not effect this interaction. Lane 1, molecular weight marker; Lane 2, 165 bp DNA; Lane 3, unlabeled Nuc165; Lane 4–6, increasing titrations of unlabeled PARP-1 with unlabeled Nuc165; Lane 7, Atto-647N labeled Nuc165; Lane 8–10, increasing titration of Alexa488 labeled PARP-1 with Atto-647N Nuc165.

F. EMSA analysis of N-Parp with NLE-Tri. NLE-Tri was incubated with N-Parp (0.8, 1, 1.2, 1.4, 1.6, and 1.8-fold excess) and analyzed on 1% agarose. Gels were stained as indicated. N-Parp binding to trinucleosomes resulted in band of slower mobility. Lane 1, Molecular weight marker (1kb); Lane 2, NLE-Tri alone; Lanes 3–8, increasing titration of N-Parp (0.8–1.8) with NLE-Tri; Lane 9, NLE-Trimer DNA (561 bp). Samples from lanes 2 and 6 were used in the AUC experiments in Figure 3D.

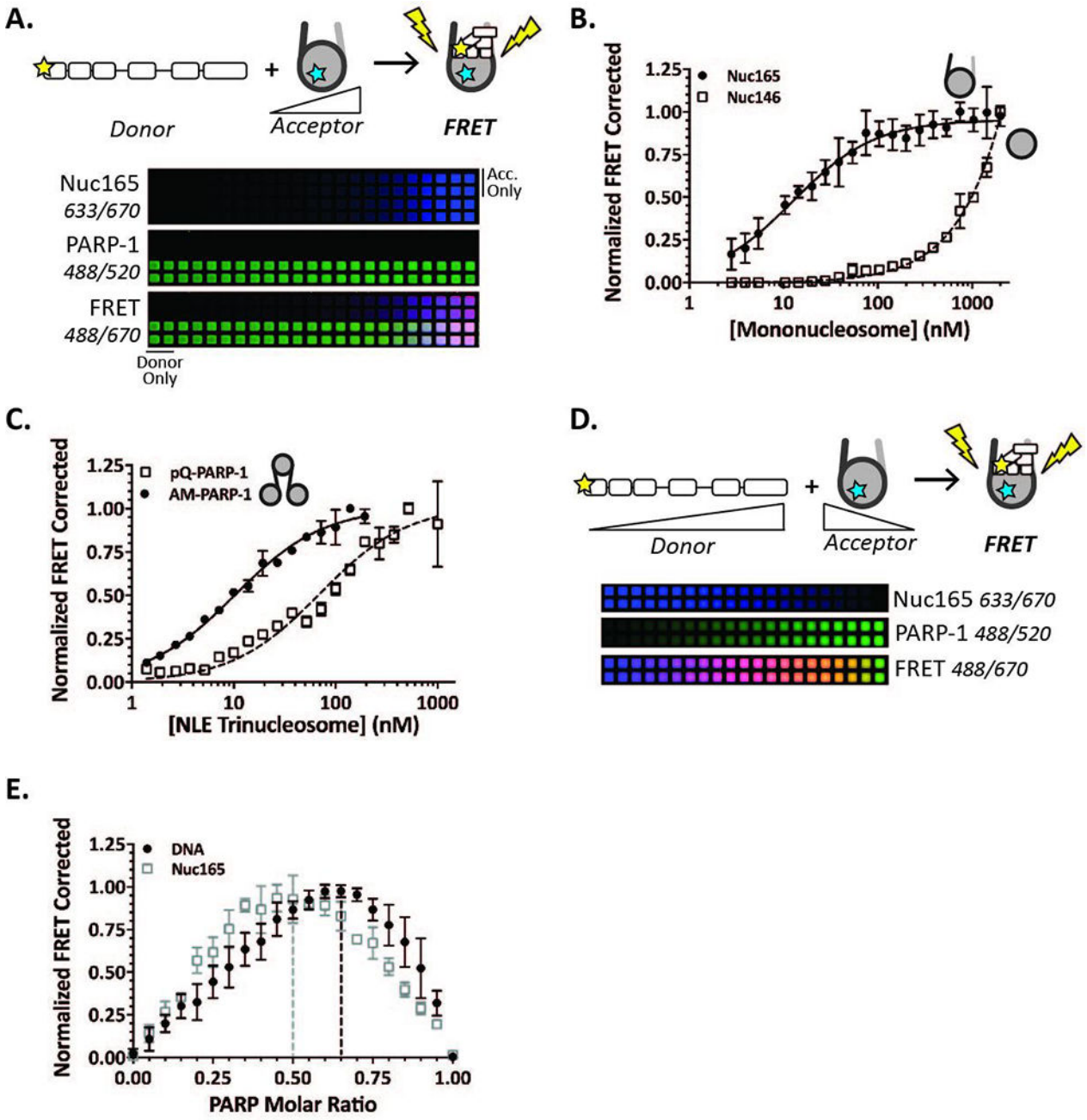

Figure 2. HIFI-FRET binding & Job plot stoichiometry assays

A. Schematic of HIFI-FRET binding assays (top) and representative FRET plate typhoon scans (bottom). Donor probe (e.g. PARP-1) is kept constant while acceptor ligand (e.g. Nuc165) is titrated. Acceptor only (acceptor + buffer) in the top two rows; donor only (donor + only) in the first two wells in the FRET series. Interaction between the two binding partners yields FRET.

B. A representative binding curve of PARP-1 binding mononucleosomes with and without DNA linker ends. PARP-1 binds Nuc146 (□, dashed line) with weak affinity (> 500 nM) and no saturatable plateau. PARP-1 binds Nuc165 (●) with low nanomolar affinity (~2 nM).

C. Representative binding curve for Pre-Quenched PARP-1 (pQ) (●) and AM-PARP-1 (□, dashed line) to NLE-Tri. PARP-1 binds tightly to NLE-Tri (~5 nM); the affinity weakens 20-fold when PARP-1 is automodified (~101 nM). *Note that panel 2C is reused from a previous publication (3).*

D. Schematic of Job plot stoichiometry experimental set up (top) and representative plate typhoon scans (bottom). The donor probe (here, PARP-1) is incrementally increased while acceptor ligand (here, Nuc165) is incrementally decreased keeping the overall molar ratio equal to one. Interaction between the two binding partners yields FRET signal.

E. Representative Job plot stoichiometry curve for PARP-1 binding double stranded DNA (●) and mononucleosomes (□). The dashed lines indicate the peak of each curve and the ideal molar ratio. At a peak of 0.5, PARP-1 binds Nuc165 in a 1 to 1 stoichiometry. DNA binds two PARP-1 molecules (peak of 0.66).

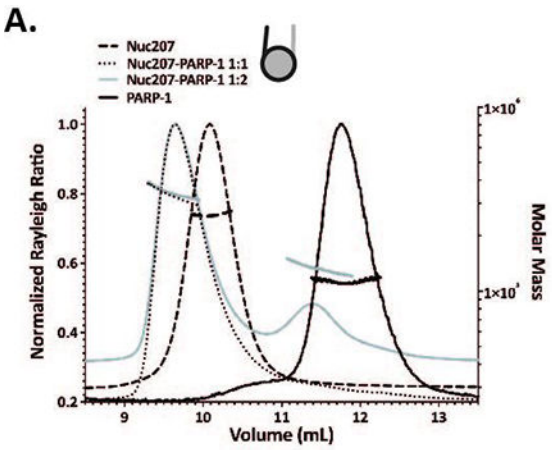

	Observed MW	Calculated MW	Error
Nuc207	2.45 x 10^5	2.36x10^5	3.7%
PARP-1	1.10 x 10^5	1.13 x 10^5	2.7%
Nuc207+ PARP-1 (1:1)	3.50 x 10^5	3.49 x 10^5	0.3%
Nuc207 + PARP-1 (1:2)	3.50 x 10^5	4.62 x 10^5	24.2%

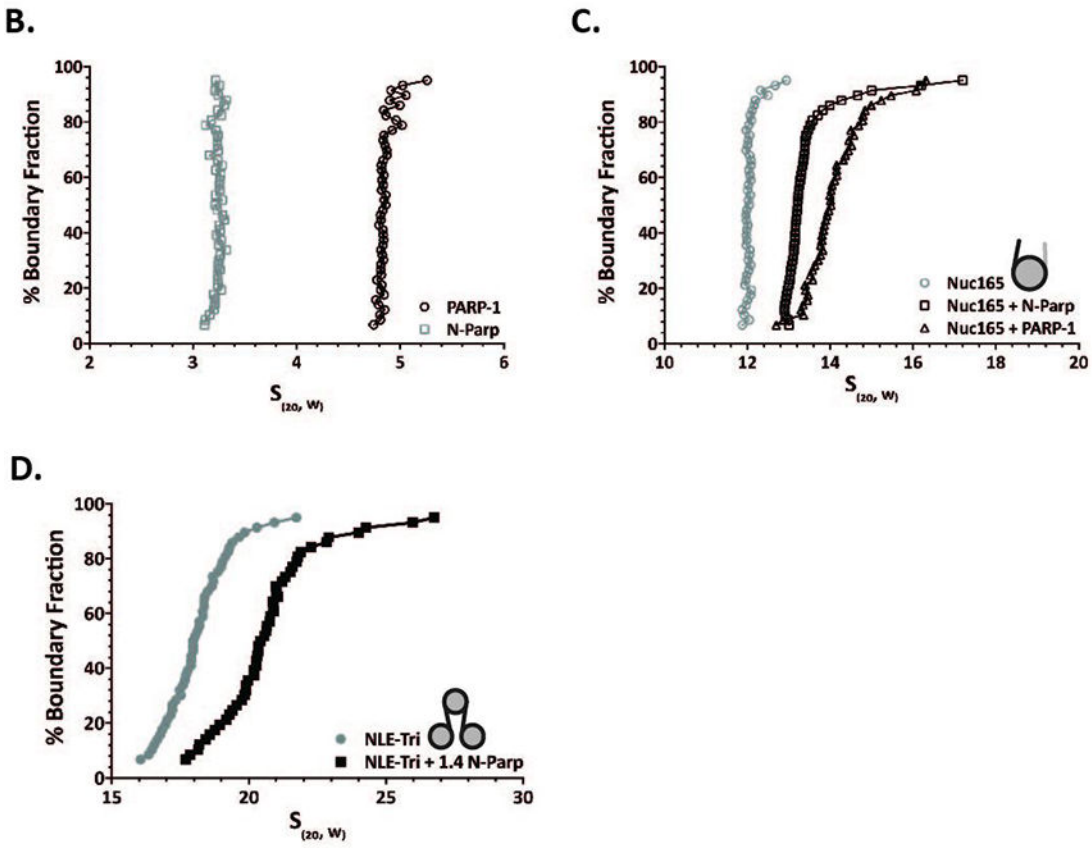

Figure 3. Solution state analysis of PARP-1 binding mono- and tri-nucleosomes

A. Analysis of PARP-1 binding mononucleosomes via size exclusion coupled multi-angle light scattering. Nuc207 forms a 1:1 complex with PARP-1 even when excess PARP-1 is added. The molecular weights for the various complexes derived are listed in the table. *Note that panel 3A figure and table are reused from (5).*

B. Analysis of PARP-1 by AUC. Sedimentation velocity profile for N-Parp (□) indicates an S_{avg} value of ~3.2S and ~5S for full length PARP-1 (○). The vertical nature of the G(s) plot indicates homogeneity of the protein samples.

C. Analysis of PARP-1 interaction with mononucleosomes via AUC. Sedimentation velocity profile for Nuc165 (○, gray) gives rise to an S_{avg} of ~12S, complex formation with N-Parp (□) results in a shift of the complex S_{avg} to ~13S; and full length PARP-1 (Δ) interaction with nucleosomes shifts the S_{avg} to ~14S.

D. Analysis of N-Parp tri-nucleosome complexes via AUC. Sedimentation velocity profile for NLE-Tri (●, gray) has an S_{avg} of ~17S, interaction with N-Parp (■) results in an S_{avg} of ~21S.

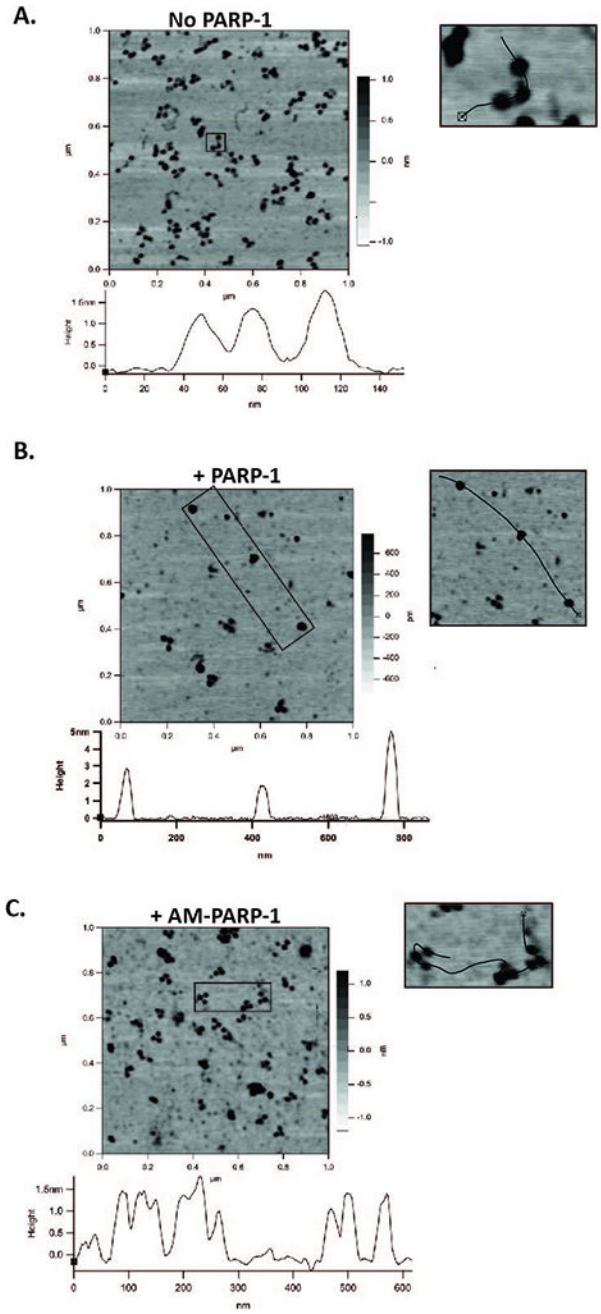

Figure 4. Atomic force microscopy of trinucleosomes and PARP-1 trinucleosome complexes

A, B, C. AFM of NLE-Tri and PARP-1 NLE-Tri complexes. 1–1.5 μm scans are shown here. A. NLE-Tri alone; B. NLE-Tri + PARP-1; C. NLE-Tri + automodified PARP-1 (AM-PARP-1). Height profiles of selected particles are shown underneath each image. In the absence of PARP-1, trinucleosomes have a height profile of 1.5–2 nm but in the presence of PARP-1, the trinucleosomes are compacted (height profiles increase to 3–5 nm). Compaction is alleviated by automodification of PARP-1 and release from chromatin (height profiles similar to no PARP-1). *Note that panels 4A-C are reused from a previous publication (3).*

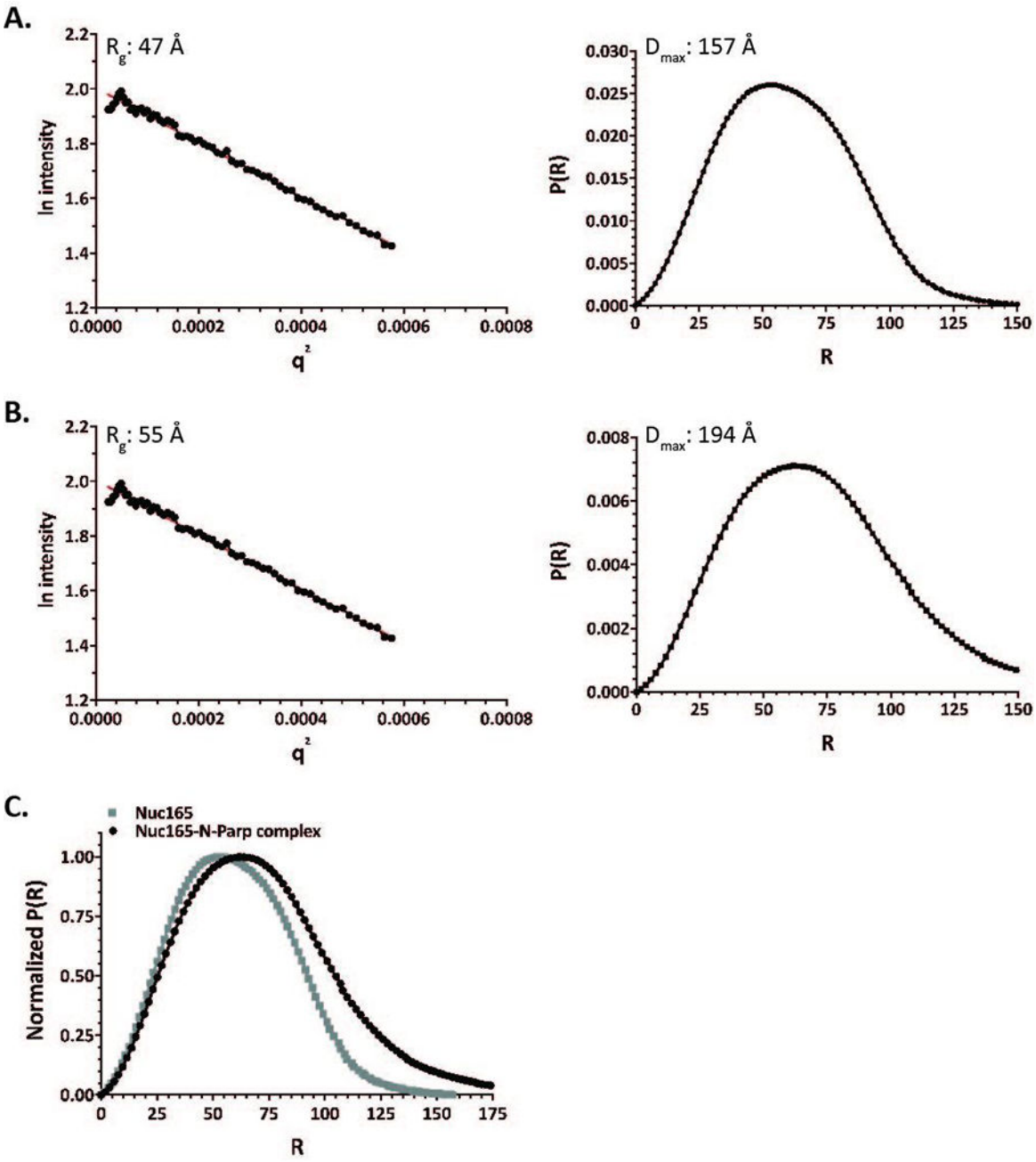

Figure 5. Small angle x-ray scattering (SAXS) of N-Parp – mononucleosome complex

A. SAXS data for the mononucleosome. Left panel - Guinier plot for data acquired for Nuc165 indicates a radius of gyration (R_g) of 47 Å. Right panel - P (R) function plot for Nuc165 indicates a maximum dimension (D_{max}) of ~157 Å.

B. SAXS data for N-Parp mononucleosome complex. Left panel - Guinier plot for Nuc165-N-Parp complex indicates an R_g of ~55 Å. Right panel - P (R) function plot for mononucleosomes indicates a D_{max} of ~194 Å.

C. Overlay of the normalized P(R) function plot for Nuc165 (■, gray) and N-Parp+Nuc165 complex (●, black). Shift is indicative of an increase in size potentially indicative of PARP binding.

Table

	Observed MW	Calculated MW	Error
Nuc207	2.45×10^5	2.36×10^5	3.7%
PARP-1	1.10×10^5	1.13×10^5	2.7%
Nuc207+ PARP-1(1:1)	3.50×10^5	3.49×10^5	0.3%
Nuc207+PARP-1 (1:2)	3.50×10^5	4.62×10^5	24.2%